



Published in final edited form as:

*Biochemistry*. 2013 July 23; 52(29): . doi:10.1021/bi4005254.

## Organization of F-actin by Fesselin (avian smooth muscle synaptopodin 2)

Mechthild M. Schroeter<sup>1</sup>, Albina Orlova<sup>2</sup>, Edward H. Egelman<sup>2</sup>, Brent Beall<sup>3</sup>, and Joseph M. Chalovich<sup>4</sup>

<sup>1</sup>Institute of Vegetative Physiology University of Cologne, Robert Koch Strasse 39, D-50931 Cologne, Germany Phone: +49-221-478-7855 Fax: +49-221-478-3538

<sup>2</sup>Department of Biochemistry and Molecular Genetics University of Virginia Box 800733 Charlottesville, VA 22908-0733 Phone: 434-924-8210 Fax: 434-924-5069

<sup>3</sup>Department of Biotechnology Athens Technical College 800 US HWY 29N Athens, GA 30601 Phone: 706-227-5350 Fax: 706-425-3104

<sup>4</sup>Department of Biochemistry & Molecular Biology Brody School of Medicine at East Carolina University 600 Moyer Blvd. Greenville, NC 27834-4300, USA Phone: 252-744-2973 chalovichj@ecu.edu

### Abstract

Fesselin or avian synaptopodin 2 is a member of the synaptopodin family of actin binding proteins. Fesselin promotes G-actin polymerization and the formation of large actin complexes that can be collected by centrifugation at low speed. Because of the potential role of fesselin in some cancers and its effects on actin we further investigated the effect of fesselin on actin. Fesselin initiated actin polymerization at a variety of conditions including the virtual absence of salt. Actin filaments formed at low salt in the presence of fesselin were similar to filaments polymerized in the presence of 100 mM KCl. In both cases the filaments were long and straight with a common orientation. Highly ordered actin bundles formed with increasing times of incubation. Blockers of actin growth at the barbed end (cytochalasin D and CapZ) did not prevent fesselin from polymerizing actin. Low concentrations of fesselin increased the critical concentration of actin. Both observations are consistent with preferential growth at the pointed end of actin filaments. These results indicate a role of fesselin in organizing cellular actin. These and other results indicate that fesselin is part of a cellular actin organizing center.

---

Actin is a major component of muscles and forms the thin filaments over which myosin moves. Actin is also present in non-muscle cells where it performs diverse critical functions including actin directed and actin-myosin driven movements. The many roles of actin are in part the result of the different structures that actin can form in conjunction with the cadre of cellular actin accessory proteins (1). Monomeric actin is stimulated to polymerize by nucleating factors. Some actin binding proteins induce actin to form various types of bundles or networks. Other proteins stabilize monomeric actin, cap actin filaments or sever actin filaments. The synaptopodin family of actin binding proteins nucleates actin filament formation and produces higher order structures that have not been identified. This manuscript describes the structure of the actin-fesselin complex at the level of electron microscopy and explores the possibility that fesselin affects the two ends of actin filaments differently.

The synaptopodin family (2) consists of proline-rich basic proteins that bind to actin (3), (4, 5). Three members of the synaptopodin family have been identified and each has multiple splice forms (2). Fesselin, or avian synaptopodin 2 (6,7) is the most readily purified form of synaptopodin family members (5, 8) and is the subject of the work described here. Fesselin consists of a mixture of two polypeptides with a molecular weight of 79 and 102 kDa. Both polypeptides contain the myopodin core region common to all synaptopodin 2 members (2).

Antibodies directed against synaptopodin 2 decorate Z-lines of rat skeletal and human heart muscle (4) and dense bodies of smooth muscle cells (9). These locations suggest that one function of synaptopodin 2 is to participate in organization of highly organized cellular actin structures (2).

The known functions of fesselin/synaptopodin 2 are consistent with a close association with actin. In particular, fesselin facilitates actin polymerization by accelerating the rate of nucleation (10). That activity is inhibited by  $\text{Ca}^{2+}$ -calmodulin (11). We now show that actin filaments formed by the addition of fesselin to G-actin are unremarkable in appearance at the level of electron microscopy.

Upon standing, mixtures of fesselin and F-actin become turbid and fesselin-actin complexes can be collected by low speed sedimentation (5). We show here that these complexes consist of tightly packed and ordered bundles with uniform polarity.

Our earlier study suggested that fesselin did not alter the critical concentration of actin (10). However, with lower concentrations of fesselin we now see an increase in the critical concentration. Other evidence will be shown that fesselin facilitates growth preferentially at the pointed or slow growing end of actin filaments. This preferential growth might explain the order and uniform polarity of fesselin induced actin bundles.

## Experimental Procedures

### Protein Preparations

Fesselin was purified from turkey gizzards by our published method (5) with additional gel permeation chromatography on a Superose™ 6 (GE Healthcare, Piscataway, NJ) column. Actin was purified from rabbit back muscle (12, 13). In some studies, F-Actin was modified with N-(1-pyrenyl)iodoacetamide (Molecular Probes) at pH 7.6 (14). G-actin was prepared by exhaustive dialysis of F-actin against G-actin buffer (5 mM Tris pH 8.0, 0.1 mM  $\text{CaCl}_2$ , 0.2 mM ATP, and 1 mM dithiothreitol). The G-actin was purified by gel filtration chromatography over Superdex™ 200 or Superose™ 6. Skeletal myosin was prepared from rabbit back muscle (15). Myosin-S1 was made by digesting myosin with chymotrypsin (Worthington Biochemical, Freehold, NJ) (16). Heterodimeric CapZ with the subunits alpha 1 beta 1 was expressed in BL21(DE3) bacteria from a pET3d plasmid, a gift of John Cooper, Washington University, St. Louis (Addgene plasmid #13451). Expression and purification of CapZ was performed according to Soeno et al. (17).

### Preparation of samples for electron microscopy

Column purified G-actin was flash frozen and stored at  $-80^\circ\text{C}$  in small aliquots. Directly before use the aliquots were thawed and centrifuged for 45 min at  $4^\circ\text{C}$  at 100,000 rpm in a TLA 120.1 rotor. The upper 60% of the supernatants were used for polymerization. Bound  $\text{Ca}^{2+}$  in G-actin was exchanged with  $\text{Mg}^{2+}$  (18) immediately before mixing with fesselin at different ratios that was in a buffer containing 10-100 mM NaCl, different buffers, pH 7.0-7.2, and 1 mM dithiothreitol. The mixture was loaded onto glow-discharged carbon coated grids. The sample was blotted off after the appropriate incubation time and the specimens were negatively stained with 2% uranyl acetate (19). Images were obtained on a

T-12 (FEI) electron microscope with an accelerating voltage of 80kV, at a magnification of 30,000 times. Electron micrographs were scanned with a Nikon-Super Coolscan-9000 digital camera.

### Critical concentration measurements

Freshly column purified G-actin (20% pyrene labeled) was polymerized. Following ATP-removal the F-actin was serially diluted into G-actin buffer in absence or presence of fesselin. The concentrations of both, actin and fesselin were varied to keep the free fesselin concentration constant in each experiment. Reactions were incubated at 20°C overnight. Fluorescence measurements were made on an Aminco Bowman II luminescence spectrometer (Thermo Electron, Madison, WI) at 25°C with excitation at 365 nm (bandpass 1nm) and emission at 407 nm (bandpass 4 nm). All fluorescence measurements were made in triplicate. The measured fluorescence was plotted against the used actin concentration. The abrupt change in slope gave the critical concentration.

### Results

Figure 1A shows the time course of pyrene labeled G-actin fluorescence at very low ionic strength. In the absence of fesselin, G-actin was stable under these conditions and no observable increase in fluorescence occurred over 150 seconds. Addition of fesselin to 0.075  $\mu$ M resulted in a rapid increase in pyrene fluorescence that indicates actin polymerization (20). Figure 1B shows an experiment performed in the presence of 100 mM KCl. Under these conditions G-actin polymerized at a slow rate (lowest curve). Fesselin accelerated polymerization 4-fold and 11-fold at 0.075 and 0.27  $\mu$ M, respectively. Higher concentrations of fesselin were required in the presence of KCl presumably because of a reduced affinity of fesselin for actin.

The structure of actin filaments polymerized with fesselin was determined by electron microscopy. Figs. 2A and B show filaments formed at very low ionic strength, and prepared at 30 seconds and 2 minutes, respectively, after adding fesselin. The incubation times were measured after the protein mixture was spotted onto the microscopy grids. Actin filaments and short bundles were observed at 30 seconds. Long actin filaments and larger bundles were seen at 2 minutes.

Panels 2C and D show actin filaments formed in the presence of 100 mM KCl. After 2 minutes many long actin filaments were seen and in many cases the filaments formed bundles. At longer times (Fig. 2D) the number of individual actin filaments decreased as the number of large actin bundles increased. Exceptionally well ordered bundles such as those shown in Figure 2D were common. Decoration of actin filaments by fesselin was not visible.

Complexes of actin and moderate concentrations of fesselin (0.02-0.2  $\mu$ M) were often found as loosely packed parallel filaments (Figure 3A). Those loose bundles show evidence of non-random initiation points. Increasing order was seen with increasing incubation times (Figure 3B). Figure 3C shows well ordered bundles in addition to free actin filaments. Densely stained regions, from which actin filaments extended, were occasionally observed when the ratio of fesselin to actin was high. Figure 4 shows one view of such an organization center at two magnifications. Actin filaments were parallel as they passed over the aggregate suggesting an organization similar to that described for Z-disk by Tskhovrebova (21).

Actin bundles formed in the presence of fesselin were decorated with S1 to determine the orientation of the actin filaments. Figure 5 shows that all of the visible actin filaments within

a bundle have the same polarity. That is, the S1 “arrowheads” point in the same direction, as indicated on the figure, and are always directed to central dense regions of the bundles.

In order to address the reason for the common start/termination points of actin filaments within a fesselin induced bundle we explored the possibility that fesselin blocks one end of an actin filament. We determined if fesselin could promote actin filament growth in the presence of cytochalasin B, a known barbed end blocker (22).

Figure 6A, curve 1 shows that actin polymerization was very slow at low ionic strength with 1 mM  $Mg^{2+}$  and was reduced to 75% of the initial rate by the addition of 0.093  $\mu$ M cytochalasin B (curve 2). Upon adding fesselin to G-actin in the absence of cytochalasin B there was a 16-fold increase in the initial rate of polymerization (curve 6). Addition of 0.04  $\mu$ M cytochalasin B had no effect on the polymerization curve of actin-fesselin (overlap with curve 6, not shown). Higher concentrations of cytochalasin B (0.093  $\mu$ M curve 5 and 0.264  $\mu$ M curve 3) produced a more pronounced flattening of the polymerization curve but did not affect the initial slope of fluorescence change vs. time. Figure 6B shows that fesselin was able to stimulate actin polymerization when the barbed/fast growing end was blocked with a concentration of cytochalasin B 1000-fold greater than that in figure 6A. Figure 6C shows that at higher ionic strength fesselin continued to induce polymerization in the presence of a very high concentration of cytochalasin B.

We studied the ability of fesselin to stimulate actin polymerization with another barbed end blocker, CapZ ( $\beta$ -actinin) using electron microscopy. G-actin was incubated with CapZ and then mixed with fesselin. Actin remained primarily in the globular state in the presence of CapZ and absence of fesselin (Figure 7A). However, the addition of fesselin resulted in rapid polymerization and bundle formation (Figure 7B). We observed that although fesselin induced actin growth in the presence of CapZ, higher concentrations were required than in the absence of this blocker.

The previous results indicate that fesselin is either able to displace very high concentrations of agents that block the fast growing end of actin filaments or else fesselin is able to stimulate growth from the slow growing, pointed end. The prediction for the latter case is that the critical concentration for filament growth should increase.

The critical concentration of actin was measured at low fesselin concentrations where bundling of actin filaments was not observed. Figure 8 shows critical concentration determinations made with pyrene labeled actin to monitor actin filament formation. The concentration of fesselin was adjusted at each actin concentration to give a constant free fesselin concentration. The concentration of free fesselin was calculated from the McGhee & von Hippel equation (23) using the program MLAB (Civilized Software, Bethesda USA) and the following constants: single site association constant =  $2 \times 10^6 M^{-1}$ , cooperativity parameter = 1.7 and the number of actin protomers covered by a single fesselin molecule = 4 (5). Under these conditions, fesselin increased the critical concentration of actin from about 0.26  $\mu$ M to about 0.44  $\mu$ M, a value closer to that for growth at the pointed end.

## Discussion

The cellular localization of avian fesselin (synaptopodin 2) in Z-disks and dense bodies together with its stimulating effect on actin polymerization suggests that fesselin is part of an actin organization nucleation complex. The present results support that idea.

Actin filaments formed in the presence of fesselin had the typical appearance of actin filaments polymerized in the presence of higher concentrations of metal ions. The filaments were unbranched and otherwise unremarkable. Although binding studies show fesselin to be

bound along the filaments (5), it was invisible in the low-resolution electron microscope. Actin filaments formed with fesselin have a great tendency to form large ordered bundles with a uniform polarity. High concentrations of fesselin tended to produce short thick bundles.

G-Actin requires bound metals for polymerization (24). The high affinity site in the actin cleft between subdomains 2 and 4 (25) has a  $K_d$  of 2.6 nM for  $\text{Ca}^{2+}$  and 7.3 nM for  $\text{Mg}^{2+}$ . The 9 or so low affinity sites have  $K_d$  values of 0.15 mM for  $\text{Ca}^{2+}$  and  $\text{Mg}^{2+}$  and 10 mM for  $\text{K}^+$  (26). The high affinity site affects the nucleation rate ( $\text{Mg}^{2+}$  is faster than  $\text{Ca}^{2+}$ ) but the low affinity sites must normally be occupied for G-actin to polymerize to F-actin (24). Fesselin induced actin polymerization at a total  $\text{Mg}^{2+}$  concentration (5  $\mu\text{M}$ ) far below that required to saturate the low affinity sites essential for polymerization. The images of filaments formed under these conditions were similar to those of actin polymerized in the presence of 100 mM KCl. Metal ions induce conformational changes in G-actin that make it polymerization competent (27,28). Fesselin appears to have the same effect on actin. Several mechanisms of this effect are possible such as charge neutralization (fesselin is positively charged at intracellular pH) or by a conformational change induced by fesselin binding.

Actin filaments in fesselin-induced bundles had a constant orientation as determined by decoration with S1. One way for this to occur is for actin filaments to grow from a common initiation point. Such ordered growth would also explain the common observation of blunt ends of fesselin-actin bundles. Fesselin tends to aggregate in solution and it is possible that parallel actin filaments grow from these large complexes. Fesselin was not visible under the conditions presently used for electron microscopy. However at high fesselin concentrations we sometimes observed dense aggregates from which parallel actin bundles radiated. These structures are intriguing because of the presence of fesselin in smooth muscle dense bodies and other synaptopodin 2 members in Z-lines of striated muscle. Both structures also contain  $\alpha$ -actinin so it will be interesting to examine actin filaments formed in the presence of both fesselin and  $\alpha$ -actinin.

Fesselin induced actin filament growth appeared to occur primarily from the pointed end of actin filaments. That is, actin growth was not inhibited by barbed end blockers. Furthermore, fesselin increased the critical concentration for polymerization in a manner that suggested that barbed ends of actin filaments were capped. Thus fesselin has the appearance of a protein that is a component of an actin nucleation center and could therefore be essential for the formation of dense bodies in smooth muscle or their skeletal muscle equivalent the Z-lines. Figure 4 shows that fesselin-actin complexes sometimes resemble those structures.

Each end of an actin filament has its own critical concentration and the observed value measured at equilibrium is the average of that from the pointed and barbed ends. The critical concentration for the pointed end is generally about 0.6  $\mu\text{M}$  (29) while that at the barbed end is about 0.1  $\mu\text{M}$ . The effect of totally blocking growth at barbed ends of actin filaments is to increase the observed equilibrium critical concentration to a value equal to that for the pointed end alone. Figure 8 shows that fesselin nearly doubled the critical concentration of actin indicating preferential growth at the pointed end.

We previously were unable to observe a change in the critical concentration of actin in response to fesselin (10). Our earlier critical concentration measurements were determined with higher fesselin concentrations where actin bundling occurred. We now used much lower fesselin concentrations and maintained a constant free fesselin concentration within each series of measurements. Furthermore, we now increased the time of equilibration. These changes resulted in a more reliable determination of the critical concentration.

Figure 9 shows our tentative view of fesselin stimulation of actin filament and bundle formation. Fesselin is intrinsically disordered when free in solution but may fold when bound to a target ligand (30). A single molecule of fesselin binds to approximately 4 actin monomers (5). The nucleus is shown with a 1:3 binding stoichiometry as this is generally considered to be the nucleus size. The G-actin is initially shown in a polymerization incompetent state such as exists in the absence of divalent metals. Fesselin induces a change similar to that caused by metal binding possibly by neutralizing charges or by altering actin structure through the energy of binding. Fesselin initiated nucleation is inhibited by calmodulin bound to calcium (11). The ability of fesselin to stimulate filament growth in the presence of barbed end blockers suggests that fesselin promotes growth from the pointed end and may itself block the barbed end. Blocking the barbed end is consistent with critical concentration measurements. Actin monomers rapidly add to the pointed end of actin filaments. At sufficiently high concentrations of fesselin, the entire length of actin may be covered by fesselin. Because actin-fesselin is able to rapidly bind to actin nuclei the binding of fesselin to existing filaments may also occur in a way that leaves the barbed end free. The region of fesselin that normally binds to the barbed end of actin might then associate elsewhere such as with an adjacent actin-fesselin unit, with actin on a parallel filament or with a fesselin molecule on a parallel actin filament. We do not have experimental evidence for these various types of association. However, because fesselin is intrinsically disordered it is able to bind to several different ligand proteins Schroeter (2). As a result, fesselin may have multiple ways of binding to actin. Actin bundle formation occurs after both polymerization and the lateral binding of fesselin to actin.

There are several possible reasons for the actin bundle formation observed. Actin bundle formation can result from tethering by proteins that have multiple sites such as gelsolin (31) or those that bundle actin by virtue of formation of dimers such as is the case for  $\alpha$ -actinin (32). Recent evidence has been given that there are several actin binding sites in human myopodin (33), a close relative of fesselin. The region containing residues 269-521 can dimerize in non-reducing conditions and bundle actin (33). Therefore, bundling by binding fesselin to parallel actin filaments could occur. Basic actin binding proteins may promote bundling by charge neutralization (34). Fesselin is basic with a pI of 9.3 (5) so this mechanism is also possible. This is an interesting possibility because actin bundles formed with fesselin (i.e. Figure 2D) resemble those found with polylysine (35).

The results shown here together with the localization of avian fesselin (synaptopodin 2) in Z-disks and dense bodies and its stimulating effect on actin polymerization suggests that fesselin is part of an actin organization nucleation complex.

## Acknowledgments

†Funding source: Supported by grants NIH GM081303 to E.H.E and NIH AR35216 to J.M.C. from the National Institutes of Health to J.M.C. and the Brody Brothers Foundation (M.M.S. and J.M.C).

## Abbreviations

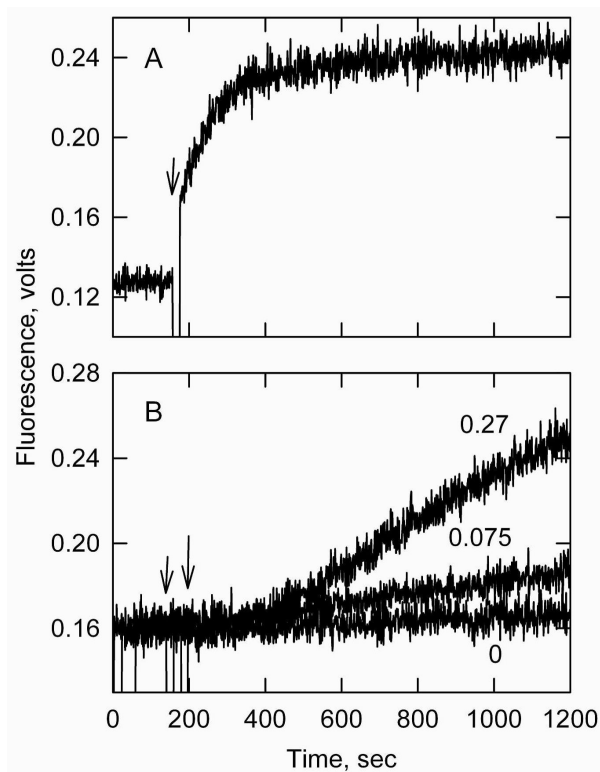
<b>S1</b>	myosin subfragment 1
<b>EGTA</b>	ethylene glycol bis( $\beta$ -aminoethyl ether)-N,N,N',N'-tetraacetic acid
<b>MOPS</b>	3-(N-morpholino)propanesulfonic acid
<b>pyrene actin</b>	actin modified with N-(1-pyrenyl)iodoacetamide

## References

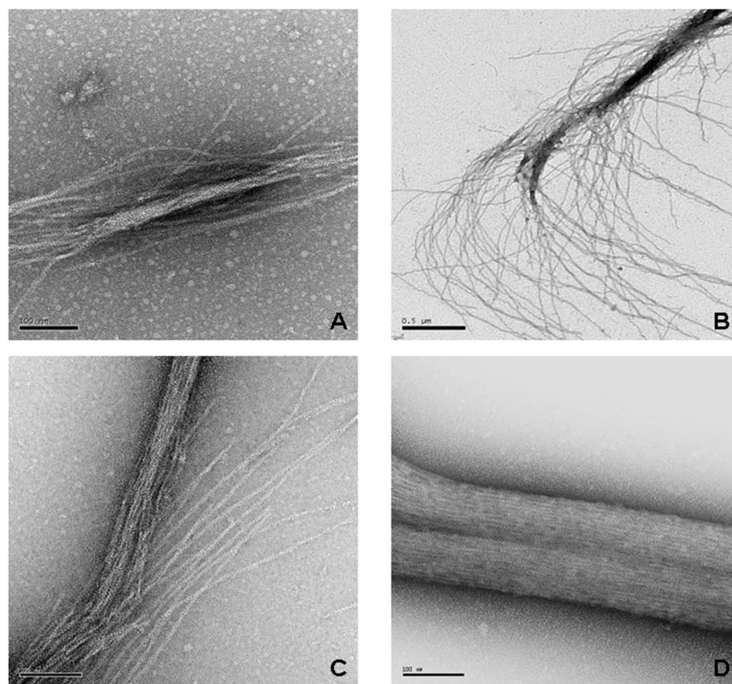
1. Pollard, TD.; Earnshaw, WC. Cell Biology. 1st ed. Saunders; Philadelphia: 2002. p. 557-577.
2. Chalovich J, Schroeter M. Synaptopodin family of natively unfolded, actin binding proteins: physical properties and potential biological functions. *Biophysical Reviews*. 2010; 2:181–189.
3. Mundel P, Heid HW, Mundel TM, Krüger M, Reiser J, Kriz W. Synaptopodin: an actin-associated protein in telencephalic dendrites and renal podocytes. *J. Cell Biol.* 1997; 139:193–204. [PubMed: 9314539]
4. Weins A, Schwarz K, Faul C, Barisoni L, Linke WA, Mundel P. Differentiation- and stress-dependent nuclear cytoplasmic redistribution of myopodin, a novel actin-bundling protein. *J. Cell Biol.* 2001; 155:393–404. [PubMed: 11673475]
5. Leinweber BD, Fredricksen RS, Hoffman DR, Chalovich JM. Fesselin: a novel synaptopodin-like actin binding protein from muscle tissue. *J. Muscle Res. Cell Motil.* 1999; 20:539–545. [PubMed: 10555072]
6. Schroeter MM, Hurley D, Chalovich JM. Multiple Isoforms of Fesselin (Avian Synaptopodin 2) are expressed in Smooth, Skeletal and Heart Muscle. *Biophys J.* 2009; 96:128a.
7. Schroeter MM, Beall B, Heid HW, Chalovich JM. The actin binding protein, fesselin, is a member of the synaptopodin family. *Biochem. Biophys. Res. Commun.* 2008; 371:582–586. [PubMed: 18457655]
8. Kolakowski J, Wrzosek A, Dabrowska R. Fesselin is a target protein for calmodulin in a calcium-dependent manner. *Biochem. Biophys. Res. Commun.* 2004; 323:1251–1256. [PubMed: 15451432]
9. Renegar RH, Chalovich JM, Leinweber BD, Zary JT, Schroeter MM. Localization of the actin-binding protein fesselin in chicken smooth muscle. *Histochem. Cell Biol.* 2009; 131:191–196. [PubMed: 18820943]
10. Beall B, Chalovich JM. Fesselin, a synaptopodin-like protein, stimulates actin nucleation and polymerization. *Biochemistry.* 2001; 40:14252–14259. [PubMed: 11714279]
11. Schroeter M, Chalovich JM. Ca<sup>2+</sup>-calmodulin regulates fesselin-induced actin polymerization. *Biochemistry.* 2004; 43:13875–13882. [PubMed: 15504050]
12. Spudich JA, Watt S. The regulation of rabbit skeletal muscle contraction. I. Biochemical studies of the interaction of the tropomyosin-troponin complex with actin and the proteolytic fragments of myosin. *J. Biol. Chem.* 1971; 246:4866–4871. [PubMed: 4254541]
13. Eisenberg E, Kielley WW. Evidence for a refractory state of heavy meromyosin and subfragment-1 unable to bind to actin in the presence of ATP. *Cold Spring Harbor Symp. Quant. Biol.* 1972; 37:145–152.
14. Brenner SL, Korn ED. On the mechanism of actin monomer-polymer subunit exchange at steady state. *J Biol. Chem.* 1983; 258:5013–5020. [PubMed: 6833289]
15. Persechini A, Hartshorne DJ. Ordered phosphorylation of the two 20,000 molecular weight light chains of smooth muscle myosin. *Biochemistry.* 1983; 22:470–476. [PubMed: 6687432]
16. Weeds AG, Taylor RS. Separation of subfragment-1 isozymes from rabbit skeletal muscle myosin. *Nature.* 1975; 257:54–56. [PubMed: 125854]
17. Soeno Y, Abe H, Kimura S, Maruyama K, Obinata T. Generation of functional beta-actinin (CapZ) in an E. coli expression system. *J Muscle Res Cell Motil.* 1998; 19:639–646. [PubMed: 9742448]
18. Zimmerle CT, Patane K, Frieden C. Divalent cation binding to the high- and low-affinity sites on G-actin. *Biochemistry.* 1987; 26:6545–6552. [PubMed: 3427024]
19. Orlova A, Egelman EH. Structural dynamics of F-actin: I. Changes in the C terminus. *J Mol. Biol.* 1995; 245:582–597. [PubMed: 7844828]
20. Cooper JA, Walker SB, Pollard TD. Pyrene actin: documentation of the validity of a sensitive assay for actin polymerization. *J Muscle Res Cell Motil.* 1983; 4:253–262. [PubMed: 6863518]
21. Tskhovrebova LA. Vertebrate muscle Z-line structure: an electron microscopic study of negatively-stained myofibrils. *J Muscle Res Cell Motil.* 1991; 12:425–438. [PubMed: 1939606]
22. Brenner SL, Korn ED. Substoichiometric concentrations of cytochalasin D inhibit actin polymerization. Additional evidence for an F-actin treadmill. *J Biol. Chem.* 1979; 254:9982–9985. [PubMed: 489616]

23. McGhee JD, von Hippel PH. Theoretical aspects of DNA-protein interactions: co-operative and non-co-operative binding of large ligands to a one-dimensional homogeneous lattice. *J. Mol. Biol.* 1974; 86:469–489. [PubMed: 4416620]
24. Estes JE, Selden LA, Kinoshita HJ, Gershman LC. Tightly-bound divalent cation of actin. *J Muscle Res Cell Motil.* 1992; 13:272–284. [PubMed: 1527214]
25. Dominguez R, Holmes KC. Actin structure and function. *Annu. Rev. Biophys.* 2011; 40:169–186. [PubMed: 21314430]
26. Carlier MF, Pantaloni D, Korn ED. Fluorescence measurements of the binding of cations to high-affinity and low-affinity sites on ATP-G-actin. *J Biol. Chem.* 1986; 261:10778–10784. [PubMed: 3814248]
27. Schüler H. ATPase activity and conformational changes in the regulation of actin. *Biochim. Biophys. Acta Protein Struct. Mol. Enzymol.* 2001; 1549:137–147.
28. Klenchin VA, Khaitlina SY, Rayment I. Crystal structure of polymerization-competent actin. *J Mol. Biol.* 2006; 362:140–150. [PubMed: 16893553]
29. Pollard TD, Blanchoin L, Mullins RD. Molecular mechanisms controlling actin filament dynamics in nonmuscle cells. *Annu. Rev. Biophys. Biomol. Struct.* 2000; 29:545–576. [PubMed: 10940259]
30. Khaymina SS, Kenney JM, Schroeter MM, Chalovich JM. Fesselin is a natively unfolded protein. *J. Proteome Res.* 2007; 6:3648–3654. [PubMed: 17676886]
31. Weeds A, Maciver S. F-actin capping proteins. *Curr. Opin. Cell Biol.* 1993; 5:63–69. [PubMed: 8383512]
32. Pollard TD, Tseng PC, Rimm DL, Bichell DP, Williams RC Jr, Sinard J, Sato M. Characterization of alpha-actinin from *Acanthamoeba*. *Cell Motil. Cytoskeleton.* 1986; 6:649–661. [PubMed: 2948678]
33. Linnemann A, Vakeel P, Bezerra E, Orfanos Z, Djinovic-Carugo K, van der Ven PF, Kirfel G, Furst DO. Myopodin is an F-actin bundling protein with multiple independent actin-binding regions. *J Muscle Res Cell Motil.* 2013; 34:61–69. [PubMed: 23225103]
34. Tang JX, Janmey PA. Two distinct mechanisms of actin bundle formation. *Biol. Bull.* 1998; 194:406–408. [PubMed: 9664675]
35. Fowler WE, Aebi U. Polymorphism of actin paracrystals induced by polylysine. *J Cell Biol.* 1982; 93:452–458. [PubMed: 7096448]

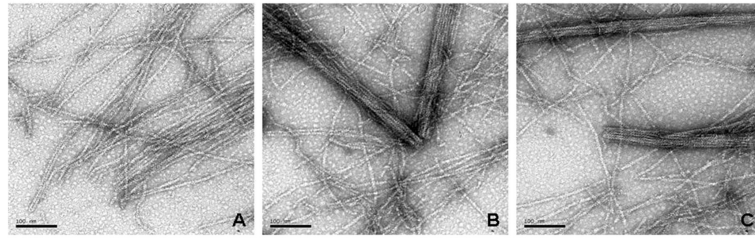




**Figure 1.** Fesselin induced actin polymerization at very low (A) and moderate (B) ionic strength. Pyrene fluorescence was monitored for 2  $\mu$ M Mg-G-actin (10% pyrene labeled) at 25  $^{\circ}$ C. Panel A conditions: 5 mM imidazole pH 7.0, 0.2 mM ATP, 0.005 mM  $MgCl_2$ . After 150 seconds fesselin was added (indicated by an arrow) to a final concentration of 0.075  $\mu$ M. Panel B: 100 mM KCl added to the buffer used in “A”. Fesselin was added as indicated to give either 0.075  $\mu$ M (short arrow) or 0.27  $\mu$ M (long arrow).

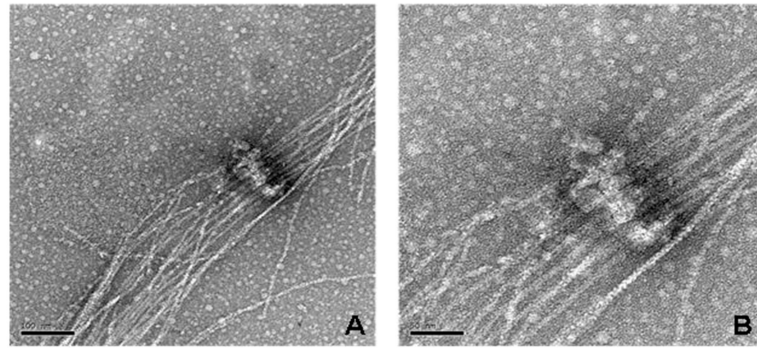


**Figure 2.** Electron micrographs of actin filaments formed in the presence of fesselin at very low ionic strength. Mg-G-actin ( $2 \mu\text{M}$ ) was placed on a carbon coated, glow discharged grid and mixed with fesselin. For (A & B) the ionic strength was 12 mM and the final concentrations of actin and fesselin were 1.5 and  $0.075 \mu\text{M}$ , respectively. The reactions were terminated by adding staining solution (2% uranyl acetate) after 30 sec in panel A and after 2 minutes in panel B. The scale bars represent 100 nm in panel A and 500 nm in B. In panels C & D the salt concentration was increased to 100 mM KCl and the final concentrations of actin and fesselin were 5 and  $0.01 \mu\text{M}$ , respectively. The reactions were stopped after 2 min in C and 10 min in D. The scale bars in panels C & D represent 100 nm.

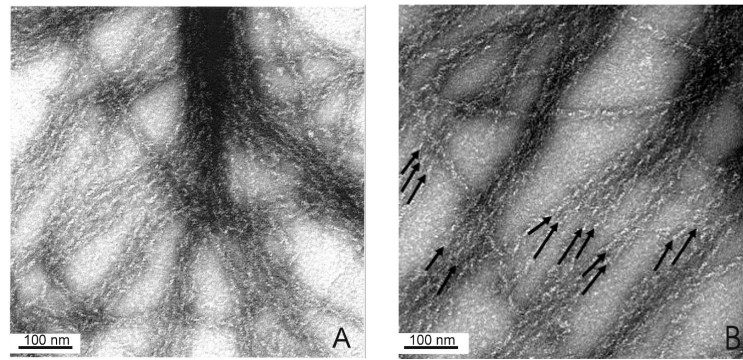


**Figure 3.**

Images of bundle formation formed with  $0.02\mu\text{M}$  fesselin and  $2\mu\text{M}$   $\text{Mg}^{2+}$ - G-actin. Fesselin and actin were mixed in a buffer containing 5 mM phosphate, pH 7.2, 0.2 mM  $\text{MgCl}_2$ , 0.2 mM EGTA, 0.2 mM dithiothreitol. KCl was added after 1 minute to a final of 100 mM. After another minute the samples were spotted onto grids. The samples were incubated on the grids for 20 sec before blotting and fixing. The scale bar represents 100 nm.

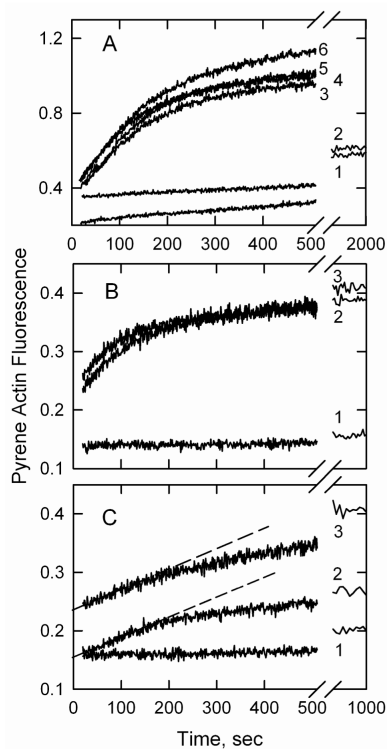


**Figure 4.** Fesselin complexes form organizing centers for actin. Polymerization of 1.5  $\mu\text{M}$  Mg-G-actin was induced by 0.075  $\mu\text{M}$  fesselin. The ionic strength of the reaction mixture was 12 mM. The reaction was stopped after 30 seconds. The scale bar in panel A represents 100 nm and that in B represents 50 nm. The conditions were the same as those in Figure 2 A & B.



**Figure 5.**

S1 decoration of actin within a fesselin-actin bundle showing that actin filaments in a bundle have the same polarity.  $2\mu\text{M}$  of G-actin was mixed with  $0.04\mu\text{M}$  of fesselin in 40 mM KCl, 1mM  $\text{MgCl}_2$ , 5mM potassium phosphate buffer, pH 7.0. After incubation in the tube for 2-3 min the sample was applied to the grid. The complex was washed with 1-2 drops of  $1\mu\text{M}$  of S1 in the same buffer. Panels A and B are different fields of the same grid. Arrows on panel B show the polarity.

**Figure 6.**

Effect of cytochalasin B on fesselin stimulated actin polymerization at 25 °C.

Polymerization was initiated by adding  $MgCl_2$  to actin. In some experiments G-actin was pre-incubated with cytochalasin for 5 minutes before polymerization was started. Panel A: 2  $\mu M$  G-actin (5% pyrene-labeled) was polymerized in a buffer composed of 15 mM KCl, 2.8 mM Tris-HCl pH 8, 1.5 mM imidazole pH 7.0, 0.1 mM ATP, 0.1 mM  $CaCl_2$ , 1 mM  $MgCl_2$ , and 1 mM dithiothreitol. Concentrations of fesselin and cytochalasin B as indicated below:

curve	1	2	3	4	5	6
[fesselin], $\mu M$	0	0	0.15	0.15	0.15	0.15
[cytochalasin B], $\mu M$	0	0.093	0.246	0.164	0.093	0

Panel B: 2  $\mu M$  G-actin (5% pyrene-labeled) with 0  $\mu M$  (curve 1) or 0.1  $\mu M$  fesselin (curves 2-3). A high concentration of cytochalasin B (0.29 mM) was present in experiment 3. The buffer was similar to that in panel A. Panel C: Polymerization with KCl raised to 39 mM KCl. Curve 1 contained 2  $\mu M$  G-actin, curve 2 also contained 0.1  $\mu M$  fesselin and curve 3 also contained 0.29  $\mu M$  cytochalasin B.

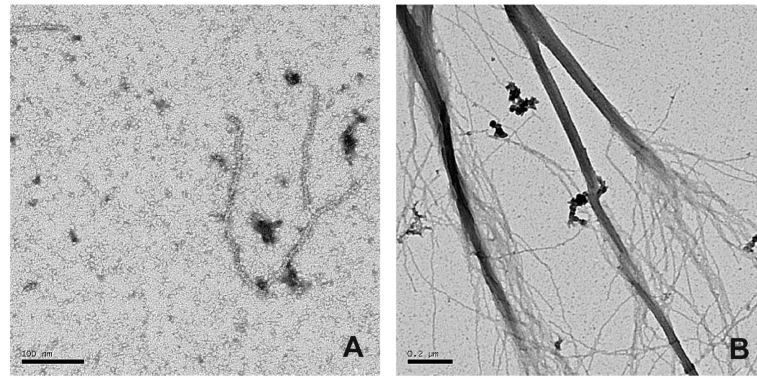


**Figure 7.** Synaptopodin 2 polymerized actin even in the presence of the barbed end blocker CapZ. Panel A shows actin polymerization in the presence of CapZ after 3 minutes of incubation. The concentrations of Mg-G-actin and CapZ were 1.5  $\mu\text{M}$  and 0.075  $\mu\text{M}$ , respectively. Panel B shows polymerization of 1.5  $\mu\text{M}$  Mg-G-actin in presence of 0.075 $\mu\text{M}$  CapZ and 0.075 $\mu\text{M}$  fesselin after 3 minutes of incubation. The ionic strength of the reaction was 90 mM.

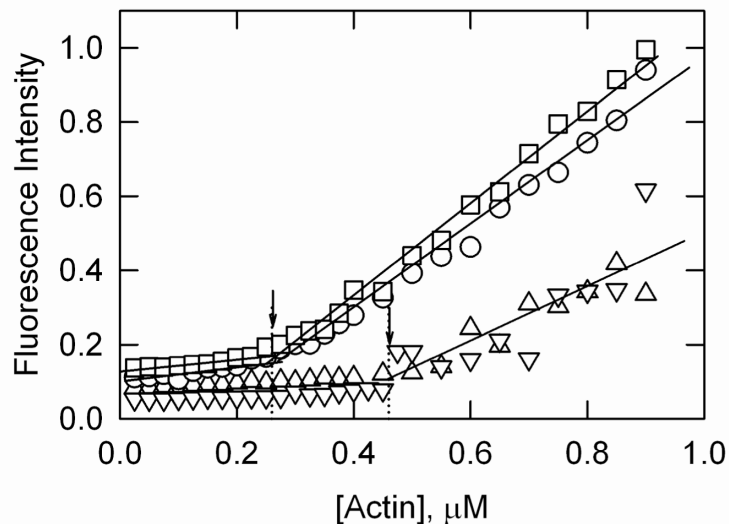


**Figure 8.**

Synaptopodin 2 increases the critical concentration of actin. Two experiments are shown in the absence of fesselin (circles and squares) and two in the presence of fesselin (triangles). Varying concentrations of column purified G-actin, 20% pyrene-labeled, were mixed with avian fesselin, keeping the free fesselin concentration constant at either  $0.01 \mu\text{M}$  (triangles up,  $\theta = 0.018$ ) or  $0.007 \mu\text{M}$  (triangles down,  $\theta = 0.013$ ). The reaction conditions were  $2 \text{ mM MgCl}_2$ ,  $100 \text{ mM KCl}$ ,  $1.5 \text{ mM imidazole pH } 7.0$ ,  $3.3 \text{ mM Tris pH } 8.0$ ,  $0.066 \text{ mM CaCl}_2$ , and  $1 \text{ mM dithiothreitol}$ . The critical concentration for actin alone (circles and squares) was  $0.26 \mu\text{M}$ . The critical concentration for actin in presence of fesselin (triangles) was between  $0.43$  and  $0.46 \mu\text{M}$ .



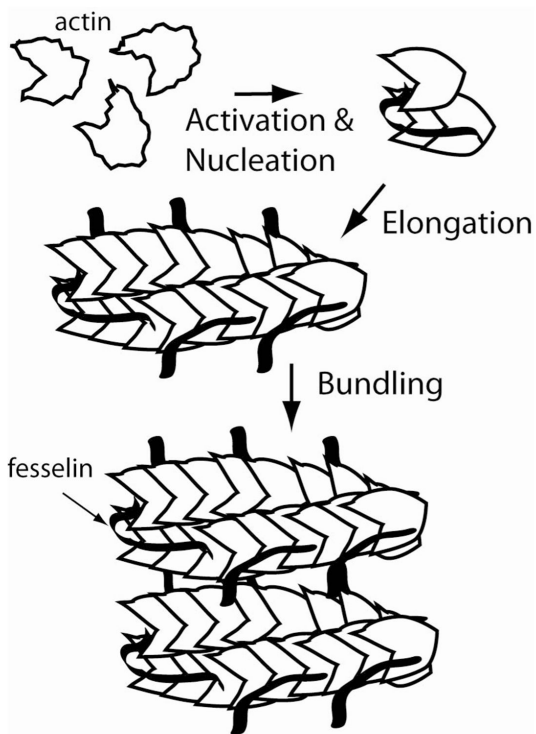


**Figure 9.**

Hypothetical model for fesselin binding, polymerization and bundling of actin. Actin monomers are drawn with barbed and pointed ends to illustrate the asymmetry of the two ends of actin filaments. Fesselin binds to about 4 actin protomers; nucleation is shown as a complex of fesselin with 3 actin monomers. Actin and actin-fesselin add rapidly to nuclei to form filaments. These filaments bundle, perhaps as a result of fesselin spanning parallel filaments.